

Synthesis, Characterization and Mechanical Properties of Geopolymer Paste



Manoj Rajak, Vikas Goel, and Baboo Rai

1 Introduction

The most utilized construction material in the world is concrete which utilizes cement as its main binding material. In recent decades, the manufacturing of cement has grown rapidly everywhere throughout the globe.

Notwithstanding, cement production has real regular issues that are of worry the world over [1]. For every ton of clinker delivered, around one ton of CO₂ is released into the air [2], which contributes just about 5–7% of overall anthropogenic carbon dioxide radiations. In the manufacturing process of cement, the principle wellsprings of gas outflows are burning of fuels and decomposition of CaCO₃ to CaO and CO₂.

Geopolymer technology has very low cost and significant contributions to reducing CO₂ emissions compared with ordinary portland cement (OPC) technology [3]. In cement production, decomposition of limestone and fossil fuels combustion results in 5–8% of global CO₂ emission. Concrete made from OPC is the most common product used around the world. In the countries where the population increases rapidly like China and India, the concrete industry is expected to grow widely [4]. The speculative preface of geopolymerization as a vital response technique of cementless concrete was developed by Davidovits in 1978, who used alkaline activators and kaolinite (Al₂Si₂O₅(OH)₄). From this point onwards, the area of cementless concrete was studied by different researchers [5, 6]. In a short period,

M. Rajak

Bureau of Indian Standards (Civil Engineering Department), Delhi 110002, India

e-mail: mkrajak.civil@gmail.com

V. Goel · B. Rai (✉)

Department of Civil Engineering, National Institute of Technology Patna, Patna 800005, India

e-mail: baboo.rai@nitp.ac.in

V. Goel

e-mail: vikasgoel.vg37@gmail.com

the researchers are magnetized to the research of low calcium FA-based geopolymer which on production emits nine times less CO₂ as compared to Portland cement [7].

Numerous tools have been used in the examination of the physical and chemical properties of FA, one such technique is quantitative X-ray diffraction (QXRD) for the mineral components [8–10]. All of these studies [8–10] reveal that “the glass chemistry of FA is the mechanism that controls to a large extent the geopolymerization process and products”. Diaz et al. [11] analysed geopolymer paste using X-ray diffraction (XRD) and Raman spectroscopy. XRD patterns for fly ash (FA) after the activation show that crystalline phases still remain, although in smaller amounts. A few authors [12, 13] studied the phase identification analysis of fly ash through QXRD and reported that the amorphous content present in the FA sample resulted from a combination of the crystalline content and the chemical composition of the sample. The same has been reported by Chen-Tan et al. [8]. The author [8] further assessed the polymerization reactivity of geopolymers coming out of the contribution of an alkaline activator to take full advantage of the reaction of the geopolymer.

XRD cannot exclusively be utilized to portray geopolymer structures because of their inherent amorphous nature; however, an in-depth understanding of how physiochemical relations between the starting materials change the rates of various reaction processes during geopolymer formation is as yet inadequate.

There are different phases in the geopolymer structure containing partly reacted and unreacted particles apart from newly formed alkali metal hydroxides, water and alkali aluminosilicate gel. A few authors [14, 15] utilized FTIR as a tool to examine the newly formed alkali alumina silicate gel (Al-rich and Si-rich) in FA-based geopolymer. One of the investigators [16] utilized Fourier transform infrared spectroscopy (FTIR) and XRD procedures to describe FA acquired from various sources to pick up a more prominent comprehension of the impact of phase composition on the reactivity, dissolution behaviour and final mechanical properties of FA-based geopolymers. Yunfen et al. [17] used XRD and FTIR to study the microstructure of geopolymers prepared using Class F FA. Characterization of geopolymers was carried out by Hamidi et al. [18] in which FA was used as raw material for geopolymer formation and FTIR analysis confirmed the same.

This paper presents the results of the experimental programme on geopolymer pastes and a brief discussion of the microstructural analysis of geopolymer paste such as XRD and FTIR. The performance of geopolymer paste with respect to compressive and transverse strength is also discussed in this paper.

2 Materials and Methods

2.1 Fly Ash

Kahalgaon Thermal Power Plant, NTPC, supplied FA samples and was used as received in this study. The physical and chemical analysis of FA powder was

Table 1 Physical properties of FA and OPC

S. No.	Physical properties	Observed value for FA
1	Specific gravity	2.2
2	Initial setting	45 min
3	Final setting	280 min
4	Consistency	35%
5	Soundness (autoclave expansion)	0.06%
6	Fineness (m^2/g)	0.368

Table 2 Chemical properties of fly ash

S. No.	Chemical properties	Observed value for FA
1	Loss of ignition	2.53
2	Silica as SiO_2	59.51
3	$SiO_2 + Al_2O_3 + Fe_2O_3$	86.85
4	Available alkalis as Na_2O	0.43
5	Reactive silica	29.32
6	Magnesium as MgO	1.97
7	Sulphate as SO_3	2.07
8	Total chloride	0.032
9	Lime reactivity	4.9 N/mm ²

performed by the manufacturer. Tables 1 and 2 represent the physical and chemical properties, respectively, and satisfy the requirements of IS 3812 (Part 1) [1]. As summarized in Table 2, FA contained 3.38 mass % as CaO and 86.85 mass % of $SiO_2 + Al_2O_3 + Fe_2O_3$. Therefore, this FA could be categorized as Class F Fly Ash according to ASTM C 618 [2].

Figure 1 shows the grain-size distribution of FA used in the experimental programme. From the figure, it can be inferred that the particle-size distribution of FA is in the portion of particles between 90 and 100 μm .

2.2 Geopolymer Synthesis

The principle materials utilized for the production of geopolymer blends were aluminosilicate materials (Na_2SiO_3) and alkali activators ($NaOH$). In the present work, FA was preferred as one of the aluminosilicate materials in geopolymer synthesis.

Sodium hydroxide pellets were taken and dissolved in distilled water to achieve 8, 10, 12, 14 and 16 molarities. Depending on the molarities of the solution, the mass of $NaOH$ solids in a solution varied.

Fig. 1 Grain-size distribution of fly ash sample

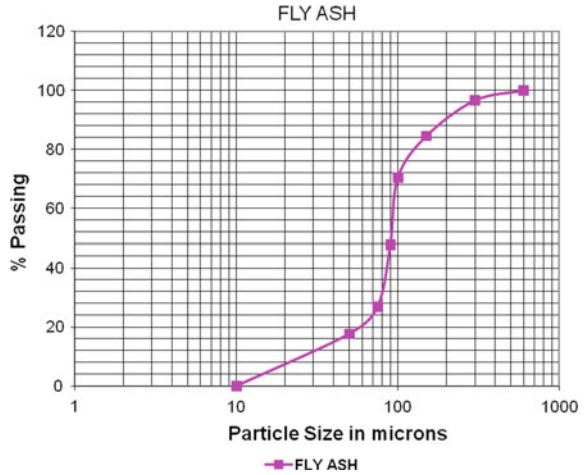


Table 3 Composition of geopolymer paste

Fly ash (gm)	Activator solution (gm)	Molarity (M)	Mass of NaOH solution (gm)	Mass of Na ₂ SiO ₃ solution (gm)
600	120	8	86	34
600	150	10	107	43
600	170	12	121	49
600	180	14	129	51
600	190	16	135	54

The preparation of sodium hydroxide solution was primed 24 h before the use because after 36 h it may terminate to semi-solid-liquid state as reported in the literature [3]. “The Sodium silicate was in solution form with SiO₂ to Na₂O ratio by mass of approximately 2” [3]. “The sodium silicate solution comprised of Na₂O = 14.7%, SiO₂ = 29.4%, and water = 55.9% by mass”. The combination of Na₂SiO₃ solution and NaOH solution was used as the alkaline liquid and was prepared 24 h before use.

Geopolymer paste was easily prepared during the mixing process as FA was effectively actuated by alkali activators. The blending procedure is continued for a couple of minutes in overhead mixes to yield a homogenous paste of geopolymer. The composition of the geopolymer paste is given in Table 3.

2.3 Curing Regimen

Preliminary investigation revealed that at room temperature, immediate hardening of fly ash geopolymer paste was not obtained. This is evident from the fact that the

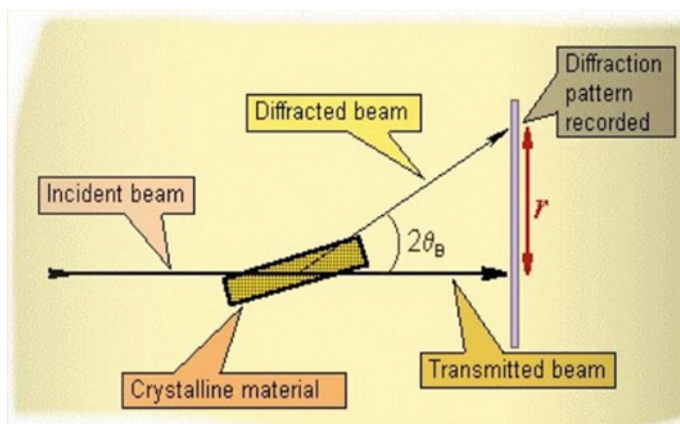


Fig. 2 Schematic representation of XRD

hardening did not occur for 24 h when the room temperature was less than 300 °C. This revelation is following the earlier researchers reported in the literature [4, 5].

FA-based geopolymer paste was placed in a universal hot oven immediately for 24 h with mould. The compressive strength test was performed after 48 h when moulds were removed from the universal hot oven and after the cubes were kept at room temperature for a further 24 h. The curing temperature was varied from 400 to 800 °C.

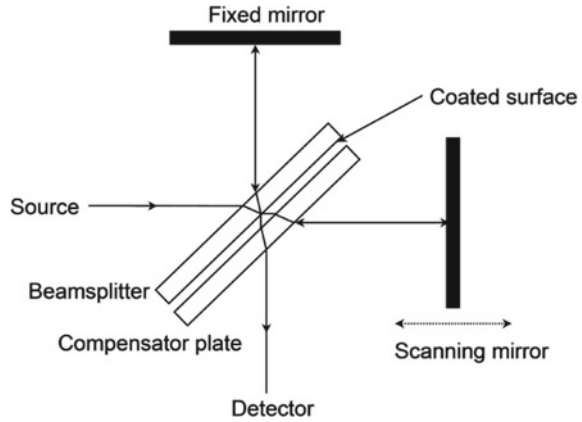
2.4 X-Ray Diffractogram

The different phases present in FA and geopolymer were observed on a device Rigaku 54 Ultima IV system using Cu K α 1 radiation ($\lambda = 1.54056 \text{ \AA}$). The phase identification analysis can be realized by comparing the spectra of patterns with JCPDS charts (01-077-0092) using the software X'pert HighScore Plus. Figure 2 presents the schematic representation of XRD.

2.5 Fourier Transform Infrared Spectroscopy

FTIR technique was used phase composition of FA-based geopolymers and also to validate the formation of geopolymers from FA. The accepted patterns in the study of the silicates help in the characterization of geopolymers. The appearance of new bands observed through FTIR helped in better understanding of formation stretching bonds like Si–O–Si, Si–O–Al, Si–O and O–Si–O.

Fig. 3 Schematic representation of FTIR



Samples were analysed using equipment of infrared spectroscopy (Shimadzu IR Affinity 1S). Schematic representation of FTIR is shown in Fig. 3. The KBr pellet technique was used to prepare the samples for infrared spectroscopy. The FTIR spectra in the wave number were recorded in the range of 400 cm^{-1} to 4000 cm^{-1} .

2.6 Compressive Strength Test

Compressive strength of geopolymer paste is determined on cubes of $7.06 \times 7.06 \times 7.06\text{ cm}$ conforming to IS:4031-Part 6-1988 [6].

2.7 Flexural Strength Test

The geopolymer paste specimens of size $40 \times 40 \times 160\text{ mm}^3$ were prepared for the flexural strength test. Flexural strength estimations were conducted using three-point bending installation utilizing four kN flexure testing machine conforming to IS: 1727-1967 [7]. The flexural strength (T) of the specimen is calculated following IS: 4031, Part-8 [8].

$$T = 0.234 \times P \quad (1)$$

where T is applied load in kN at the time of breaking and P is in kgf/cm^2 .

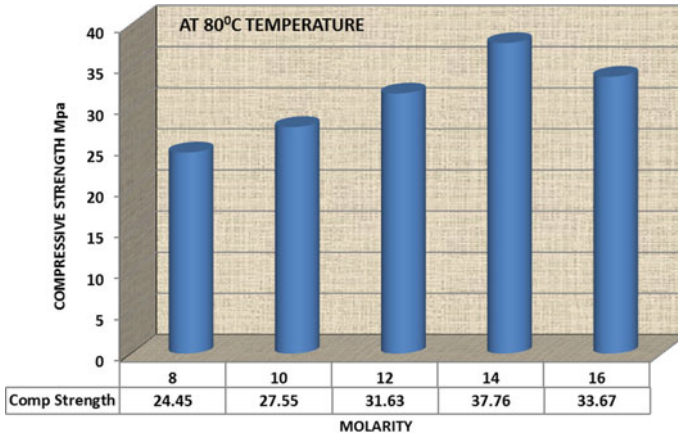


Fig. 4 Compressive strength test results at different molarity

3 Mechanical Properties

3.1 Compressive Strength

The compressive strength test results of geopolymer paste prepared by 8 M, 10 M, 12 M and 16 M of sodium hydroxide solutions are shown in Fig. 4. From the figure, it can be concluded that the compressive strength increases with an increase in molarity. The increase in compressive strength when the molarity increased from 8 to 12 M is almost 1.54 times. The sample prepared with 14 M NaOH gave the maximum compressive strength.

Further, Fig. 5 revealed that an increase in curing temperature of 40–100 °C increased in compressive strength of FA-based geopolymer paste. Further, no significant enhancement in strength was observed beyond 80 °C as there was a decrease in the rate of growth of compressive strength at 100 °C as compared to 80 °C which means that curing at 80 °C temperatures gives ideal compressive strength.

3.2 Flexural Strength Test

The flexural strength tests results of geopolymer paste are illustrated in Fig. 6. From Fig. 6, it can be inferred that the flexural strength of geopolymer paste increases with an increase in NaOH concentration. Further, at 14 M NaOH concentration, the flexural strength significantly increases. However, the flexural strength decreases at higher concentration of 16 M. This might be ascribed to the way that increasing molarity will form the separation of the active types of crude material and will produce more geopolymer gel arrangements. Nonetheless, a higher concentration of NaOH will

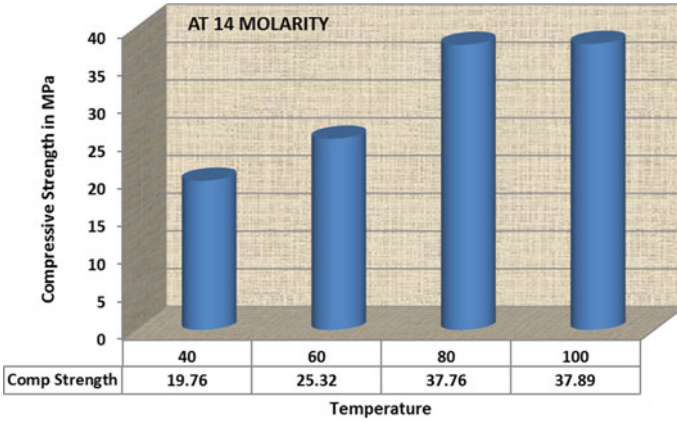


Fig. 5 Compressive strength test results at different temperature

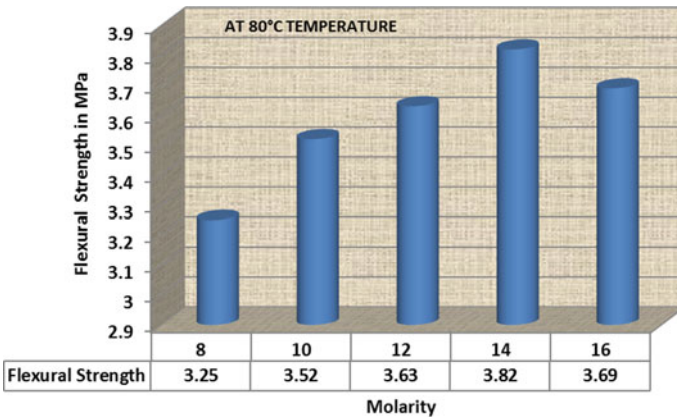


Fig. 6 Flexural strength test results at different molarity

upset the geopolymerization procedure because of the unreasonable amount OH-particles which prompt a wasteful response.

Figure 7 displays the flexural strength test results at a different temperature when the molarity is fixed at 14 M. It can be inferred that flexural strength shows an increasing trend as the temperature increases. the highest flexural strength recorded was 3.98 at 14 M and 100 °C.

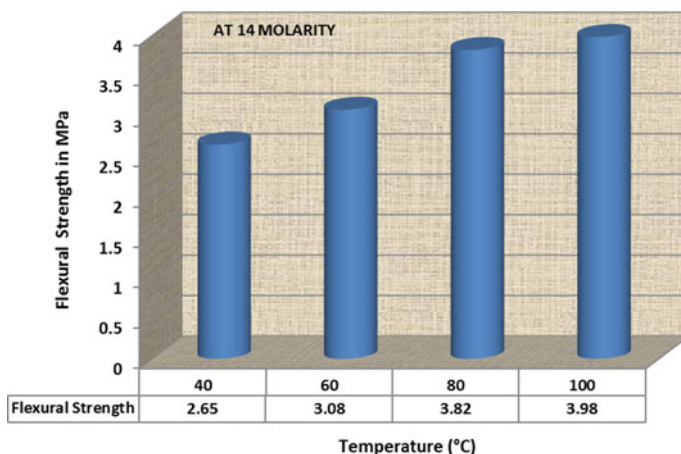


Fig. 7 Flexural strength test results at different temperature

4 Physical Properties

4.1 Phase Identification Analysis

The phase identification analysis of FA is shown in Fig. 8. A close study of the diffractogram obtained reveals a 100% peak at an angle of 26°. This peak can be attributed to the majority silica component present in the sample as it matches with the major peak of quartz crystal. The absence of broad humps in the low-angle region

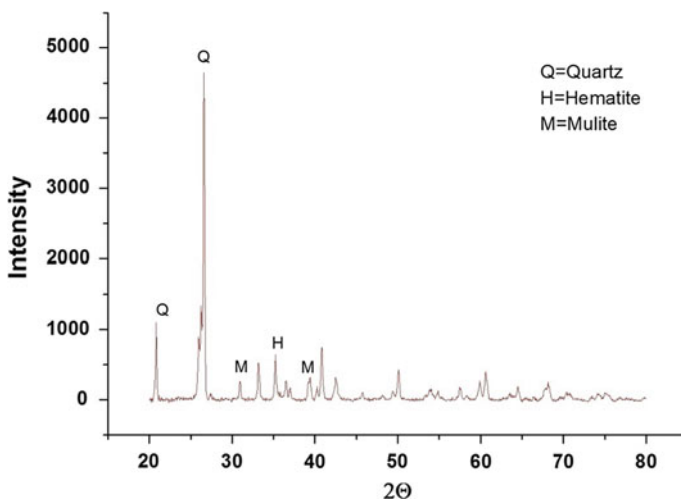


Fig. 8 Phase identification analysis of fly ash

signifies the absence of amorphous nature in the sample. The sharp peaks show good crystallinity of the sample. Along with the major quartz phase, small percentages of mullite ($3\text{Al}_2\text{O}_3 \cdot 2\text{SiO}_2$) and hematite (Fe_2O_3) were also detected in the sample and are marked in Fig. 8.

Figures 9 and 10 show the XRD pattern of the geopolymeric sample cured for 24 h. In the case of geopolymeric samples, the scans were run from 0° to 80° at an incidence angle of 2θ , with increments of 0.02° and a counting time of 2 s per

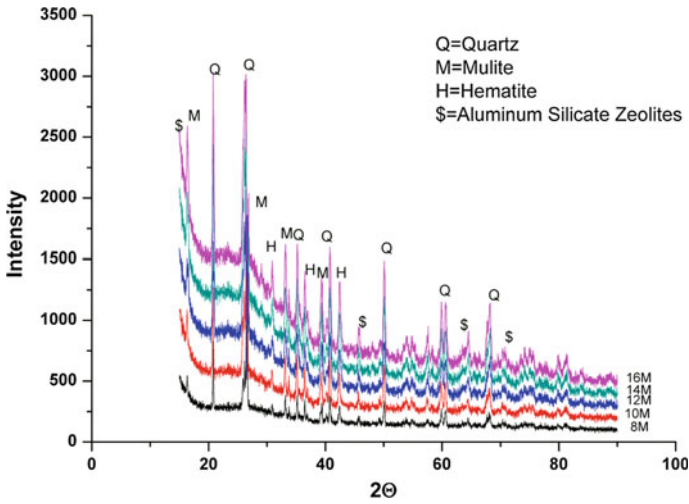


Fig. 9 XRD traces of geopolymer at different molarity

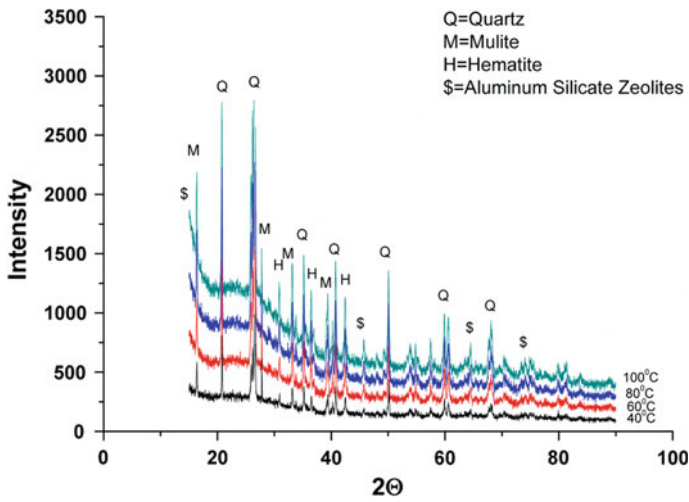


Fig. 10 XRD traces of geopolymer at different temperature

step. The patterns displayed that the geopolymer sample consisted of quartz and mullite crystals. The phase identification analysis of FA shows that the sample was amorphous and a broad peak between 21° and 35° 2θ was observed, which is a common characteristic of geopolymers [9].

From the phase identification analysis of FA (Fig. 8), a broad hump is registered between $2\theta = 26^\circ$. However, from Figs. 9 and 10 it can be seen this broad hump is marginally shifted towards higher values ($2\theta = 29^\circ$) in the phase identification analysis of the geopolymers which is indicative of the development of another amorphous alumina silicate gel in the geopolymer lattices along with the separation of the FA amorphous phase and the formation of a new amorphous phase in these materials [10, 11]. The development of new zeolite stages (aluminium silicate zeolites) is seen in the orchestrated geopolymers enrolled between $2\theta = 5^\circ$ and 15° .

The amorphous phase was overwhelming with extra pinnacles of alumina silicate mixes at NaOH concentrations of 12 M and 14 M. This marvel was the after-effect of polymerization of silicate as well as alumina silicate oligomers shaped by the disintegration of strong alumina silicate materials under solid antacid conditions [10, 11]. The improvement of the gel stage with some measure of new crystalline items demonstrated the propelled geopolymerization and quality advancement of the geopolymer paste. High molarity of NaOH would do well to dissolve FA particles and brought about improved geopolymerization. The increment in geopolymer compressive strength quality was additionally reported because of an increment in a little measure of crystalline stage [12]. The XRD traces of the 16 M sample were marginally not quite the same as those of 8 M–14 M samples. Consequent geopolymerization was obstructed bringing about low-quality advancement this might be ascribed to the way that the alumina silicate gel precipitation initiated at very early stages due to excess hydroxide ion concentration [13].

Figure 11 indicates that crystalline effects remain unaltered by varying the using temperatures and follow much the same trend which again signifies that structural integrity is affected only by changes made within the amorphous gel structure of geopolymers.

4.2 FTIR Spectroscopic Study

According to the literature [14], the strong peak at $\sim 1000\text{ cm}^{-1}$ in the FTIR spectrum of the geopolymer sample is the fingerprint of the geopolymerization. The FTIR spectra in Fig. 11 show some noteworthy contrasts as a comparison to the end product (geopolymers) spectrum to that of the initial material (FA). From Fig. 11, it can be seen that the disappearance of the band between the region $848\text{--}668\text{ cm}^{-1}$ constitutes a sign of geopolymerization and is related to symmetric stretching vibrations of Al–O. These are connected with symmetric stretching vibrations of Si–O–T bonds. The band at 792.28 cm^{-1} are attributed to symmetrical vibrations of tetrahedral groups during the reaction are due to disappearance of AlO_4 in this region. Moreover, the

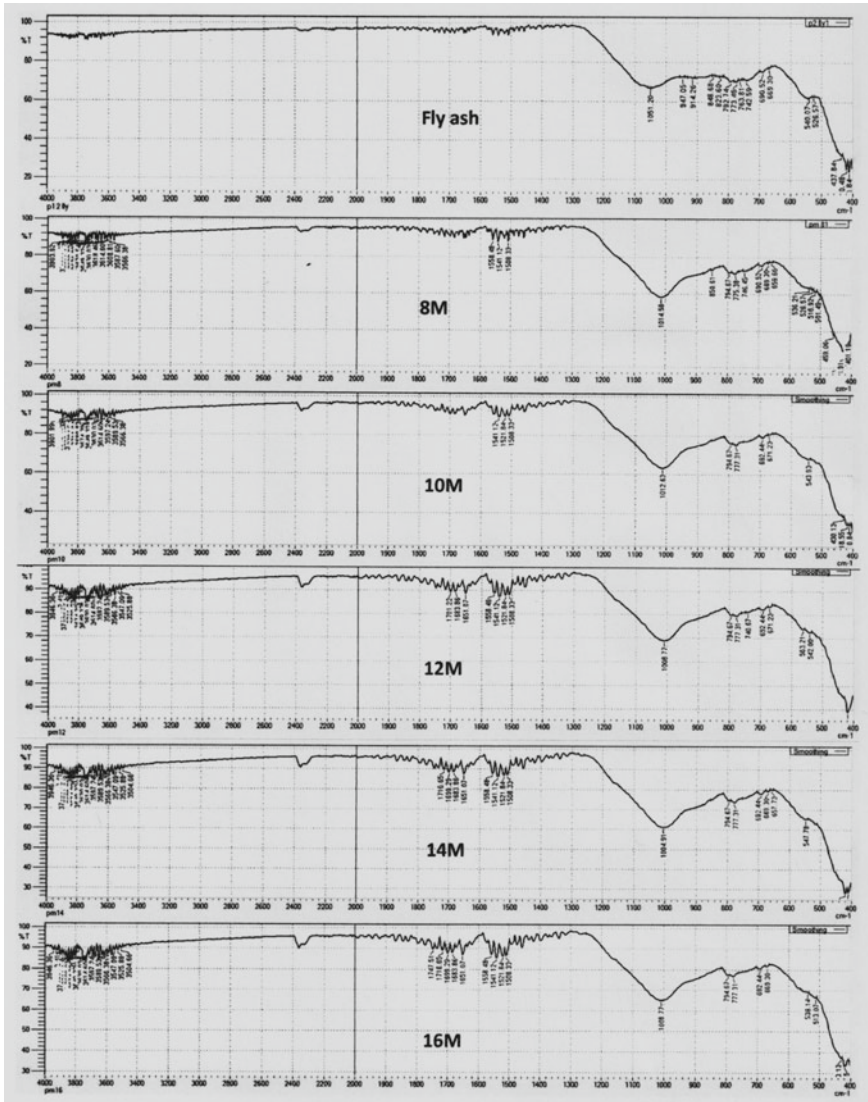


Fig. 11 FTIR spectra of fly ash and geopolymer samples at different molarity

disappearance is more prominent in the case of 14 and 16 molarity geopolymer sample.

The shifting of the band at 1051 cm^{-1} to lower frequencies ($\sim 1000\text{ cm}^{-1}$) is due to the asymmetric stretching of Si–O–Si and Al–O–Si in FA [14]. These vibrations are due to the formation of geopolymeric gels and the chemistry developing in the stages of geopolymer formation. The decreased intensity of the main bond due to the dissolution of solid silica may be ascribed to the association of alumina silicate

framework with sodium cation (Na^+). This may have caused some molecular changes in the structure while shifting to lower wave numbers [15]. A larger shift indicates a higher degree of Al penetration from the glassy part of FA into the (SiO_4) 4-skeleton as observed analogously in zeolites [16]. This observation is in good accordance with the XRD results which showed that samples of high alkalinity contain carbonate phases such as natrite, calcite and potassium carbonate.

The appearance of the band in the region of 1700 to 1650 and 3525 cm^{-1} is linked to the presence of bound water molecules and silanol group Si–OH in the geopolymer cement which may be due to bending vibrations (H–O–H) and stretching vibration (–OH), respectively. More prominent and frequent peaks were observed in the case of 14 and 16 molarity samples. The band at around 1500 to 1550 cm^{-1} suggests the presence of sodium carbonate. This may have resulted due to the reaction between sodium and atmospheric carbon dioxide [17]. This band indicates the asymmetric CO_3 stretching mode. This band was observed to be absent in the case of FA. Broader peaks at frequent intervals were observed in case of 14 M and 16 M in comparison to 8, 10, 12 molarity. Atmospheric carbonation evident at 1460 cm^{-1} has also been reported in the literature [18]. The band seen at around 540 cm^{-1} is due to double-ring linkage [19].

Figure 12 displays the FTIR spectra of 14 M geopolymer samples at different temperature. Here, it can be again seen that crystalline effects remain unaltered by varying the temperatures and follow much the same trend.

5 Summary

The quantity of Na_2SiO_3 solution in the synthesis of geopolymers demonstrated a significant influence on the strength characteristic of geopolymer. This may be attributed to the fact that Na_2SiO_3 solution controls the soluble silicate concentration and the prevalent silicate species in the geopolymeric system. Mechanical properties of geopolymers exhibited by compressive and transverse quality demonstrate that NaOH fixation offered a noteworthy effect in improving the properties where the ideal molarity of NaOH of 14 M gave improved strength properties of geopolymer.

The procedures of XRD and FTIR are of significant help and reciprocal between them, and these outcomes can be related to the physical and mechanical properties of a geopolymer. FTIR provides a tool qualitative to a semi-quantitative method for examining the reactivity of FA. The appearance of the significant band during the FTIR analysis demonstrates that the geopolymer lattice formation was successfully obtained. The rate of geopolymer formation improved with an increase in molarity of NaOH. Further, the XRD diffractogram results also demonstrated that both crystalline and amorphous phases are present in the principle geopolymeric structure.

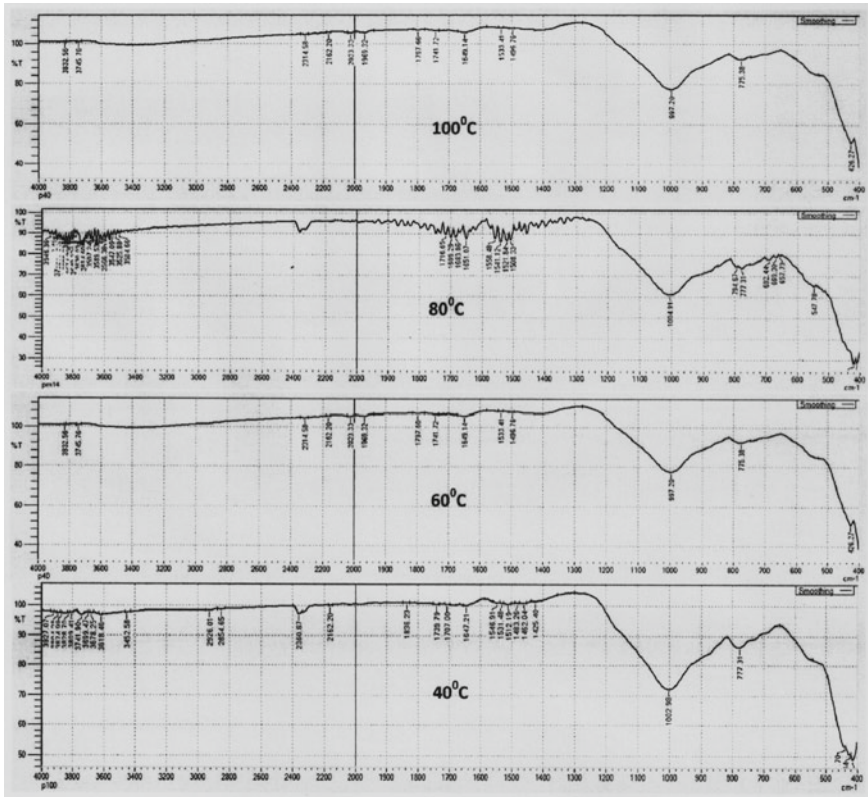


Fig. 12 FTIR spectra of geopolymer samples at different temperature

References

1. IS 3812 : Part 1 (2003) Pulverized Fuel Ash- Specification, Bur. Indian Stand
2. ASTM C 618 (2017) Standard Specification for Coal Fly Ash and Raw or Calcined Natural Pozzolan for Use in Concrete. <https://doi.org/10.1520/C0618>
3. Rai B, Roy LB, Rajjak M (2018) A statistical investigation of different parameters influencing compressive strength of fly ash induced geopolymer concrete., *Struct Concr* 1–12. <https://doi.org/10.1002/suco.201700193>
4. Davidovits J (1989) Geopolymers and geopolymeric materials. *J Therm Anal* 35:429–441. <https://doi.org/10.1007/BF01904446>
5. Phair JW, Van Deventer JSJ, Smith JD (2000) Mechanism of polysialation in the incorporation of zirconia into fly ash-based geopolymers. *Ind Eng Chem Res* 39:2925–2934. <https://doi.org/10.1021/ie990929w>
6. IS 4031 : Part 6 (1988) Methods of physical tests for hydraulic cement, Part 6: Determination of compressive strength of hydraulic cement (other than masonry cement), Bur. Indian Stand
7. IS 1727 (1967) Methods of test for pozzolanic materials, Bur. Indian Stand.
8. IS 4031 : Part 8 (1988) Methods of physical tests for hydraulic cement: Part 8 Determination of transverse and compressive strength of plastic mortar using prism, Bur. Indian Stand.

9. He J, Zhang J, Yu Y, Zhang G (2012) The strength and microstructure of two geopolymers derived from metakaolin and red mud-fly ash admixture: A comparative study. *Constr Build Mater* 30:80–91. <https://doi.org/10.1016/j.conbuildmat.2011.12.011>
10. Fernández-Jiménez A, Palomo A (2005) Composition and microstructure of alkali activated fly ash binder: Effect of the activator. *Cem Concr Res* 35:1984–1992. <https://doi.org/10.1016/j.cemconres.2005.03.003>
11. Bakharev T (2005) Geopolymeric materials prepared using Class F fly ash and elevated temperature curing. *Cem Concr Res* 35:1224–1232. <https://doi.org/10.1016/j.cemconres.2004.06.031>
12. Álvarez-Ayuso E, Querol X, Plana F, Alastuey A, Moreno N, Izquierdo M, Font O, Moreno T, Díez S, Vázquez E, Barra M (2008) Environmental, physical and structural characterisation of geopolymer matrixes synthesised from coal (co-)combustion fly ashes. *J Hazard Mater* 154:175–183. <https://doi.org/10.1016/j.jhazmat.2007.10.008>
13. Lee WKW, Van Deventer JSJ (2002) The effects of inorganic salt contamination on the strength and durability of geopolymers. *Colloids Surfaces a Physicochem Eng Asp* 211:115–126. [https://doi.org/10.1016/S0927-7757\(02\)00239-X](https://doi.org/10.1016/S0927-7757(02)00239-X)
14. Chindapasirt P, Rattanasak U, Jaturapitakkul C (2011) Utilization of fly ash blends from pulverized coal and fluidized bed combustions in geopolymeric materials. *Cem Concr Compos* 33:55–60. <https://doi.org/10.1016/j.cemconcomp.2010.09.017>
15. Hajimohammadi A, Provis JL, Van Deventer JSJ (2010) Effect of alumina release rate on the mechanism of geopolymer gel formation. *Chem. Mater.* 22:5199–5208. <https://doi.org/10.1021/cm101151n>
16. C. Panagiotopoulou, A. Asprogerakas, G. Kakali, S. Tsvilivis, Synthesis and Thermal Properties of Fly-Ash Based Geopolymer Pastes and Mortars, in: *Dev. Strateg. Mater. Comput. Des. II Ceram. Eng. Sci. Proceedings*, Vol. 32, 2011: pp. 17–28. doi:<https://doi.org/10.1002/9781118095393.ch2>.
17. Ayan E, Saatiolu Ö, Turanlı L (2011) Parameter optimization on compressive strength of steel fiber reinforced high strength concrete. *Constr. Build. Mater.* 25:2837–2844. <https://doi.org/10.1016/j.conbuildmat.2010.12.051>
18. Phair JW, Van Deventer JSJ (2002) Effect of the silicate activator pH on the microstructural characteristics of waste-based geopolymers. *Int. J. Miner. Process.* 66:121–143. [https://doi.org/10.1016/S0301-7516\(02\)00013-3](https://doi.org/10.1016/S0301-7516(02)00013-3)
19. Zaharaki D, Komnitsas K, Perdikatsis V (2010) Use of analytical techniques for identification of inorganic polymer gel composition. *J. Mater. Sci.* 45:2715–2724. <https://doi.org/10.1007/s10853-010-4257-2>